Doi K, Doi H, Noiri E, *et al.*	High-throughput single nucleotide polymorphism typing by fluorescent single-strand conformation polymorphism analysis with capillary electr ophoresis.	Electrophoresis	25	833-8	2004
Bannai M, Higuchi K, Akesaka T, *et al.*	Single-nucleotide-poly—morphism genotyping for whole-genome-amplified samples using automatedf luorescence correlation spectroscopy.	*Analytical Biochemistry*	327	215-21	2004
Omi K, Tokunaga K, and Hohjoh H.	Long-lasting RNAi activity in mammalian neurons.	*FEBS Lett.*	558	89-95	2004
Gu W, Ogose A, Kawashima H, *et al.*	High-level expression of the coxsackievirus and adenovirus receptor messenger RNA in osteosarcoma, Ewing's sarcoma, and benign neurogenic tumors among musculoskeletal tumors.	*Clin.Cancer Res.*	10	3831-8	2004
Tochigi M, Zhang X, Umekage T, *et al.*	Association of six polymorphisms of the NOTCH4 gene with schizophrenia in the Japanese population.	*Am.J.Med. Genet B.Neuropsychiatr. Genet.*	128	37-40	2004
Furuya T, Hakoda M, Tsuchiya N, *et al.*	Immunogenetic features in 120 Japanese patients with idiopathic inflammatory myopathy.	*J.Rheumatol.*	31	1768-74	2004
Hitomi Y, Tsuchiya N, Kawasaki A, *et al.*	CD72 polymorphisms associated with alternative splicing modify susceptibility to human systemic lupus erythematosus through epistatic interaction with FCGR2B.	*Hum.Mol. Genet.*	13	2907-17	2004
Akesaka T, Lee SG, Ohashi J, *et al.*	Comparative study of the haplotype structure and linkage disequilibrium of chromosome 1p36.2 region in the Korean and Japanese populations.	*J.Hum.Genet.*	49	603-9	2004
Sakurai D, Tsuchiya N, Yamaguchi A, *et al.*	Crucial role of inhibitor of DNA binding/differenttiation in the vascular endothelial growth factor-induced activation and angiogenic processes of human endothelial cells.	*J.Immunol.*	173	5801-9	2004

Ohashi J, Naka I, Patarapotikul J, *et al.*	Strong linkage disequilibrium of a HbE variant with the (AT)9(T)5 repeat in the BP1 binding site upstream of the beta-globin gene in the Thai population.	*J.Hum.Genet.*	50	7-11	2005
Tanaka G, Matsushita I, Ohashi J, *et al.*	Evaluation of microsatellite markers in association studies: a search for an immune-related susceptibility gene in sarcoidosis.	*Immunogenetics*			2005 (In press)
豊岡 照彦	心不全の重症化と, その対策	日本医事新報	4171	21-32	2004

Translocation and cleavage of myocardial dystrophin as a common pathway to advanced heart failure: A scheme for the progression of cardiac dysfunction

Teruhiko Toyo-Oka*†‡§, Tomie Kawada¶, Jumi Nakata*, Han Xie*, Masashi Urabe‖, Fujiko Masui*, Takashi Ebisawa*, Asaki Tezuka*, Kuniaki Iwasawa†‡, Toshiaki Nakajima‡, Yoshio Uehara†, Hiroyuki Kumagai**, Sawa Kostin††, Jutta Schaper††, Mikio Nakazawa‡‡, and Keiya Ozawa‖

*Department of Pathophysiology and Internal Medicine, †Health Service Center, and ‡Department of Cardiovascular Medicine, University of Tokyo, Tokyo 113-0033, Japan; ¶Division of Pharmacy and ‡‡Department of Medical Technology, Niigata University, Niigata 951-8520, Japan; ‖Division of Gene Therapy, Jichi Medical School, Tochigi 329-0498, Japan; **Department of Pharmacology, Gunma University, Maebashi 371-8511, Japan; and ††Department of Experimental Cardiology, Max Planck Institute, Bad Nauheim 61231, Germany

Communicated by Setsuro Ebashi, Okazaki National Research Institutes, Okazaki, Japan, March 25, 2004 (received for review January 24, 2004)

Advanced heart failure (HF) is the leading cause of death in developed countries. The mechanism underlying the progression of cardiac dysfunction needs to be clarified to establish approaches to prevention or treatment. Here, using TO-2 hamsters with hereditary dilated cardiomyopathy, we show age-dependent cleavage and translocation of myocardial dystrophin (Dys) from the sarcolemma (SL) to the myoplasm, increased SL permeability *in situ*, and a close relationship between the loss of Dys and hemodynamic indices. In addition, we observed a surprising correlation between the amount of Dys and the survival rate. Dys disruption is not an epiphenomenon but directly precedes progression to advanced HF, because long-lasting transfer of the missing *δ-SG* gene to degrading cardiomyocytes *in vivo* with biologically nontoxic recombinant adenoassociated virus (rAAV) vector ameliorated all of the pathological features and changed the disease prognosis. Furthermore, acute HF after isoproterenol toxicity and chronic HF after coronary ligation in rats both time-dependently cause Dys disruption in the degrading myocardium. Dys cleavage was also detected in human hearts from patients with dilated cardiomyopathy of unidentified etiology, supporting a scheme consisting of SL instability, Dys cleavage, and translocation of Dys from the SL to the myoplasm, irrespective of an acute or chronic disease course and a hereditary or acquired origin. Hereditary HF may be curable with gene therapy, once the responsible gene is identified and precisely corrected.

Despite the steady progress of pharmaceutical therapy, it is still difficult to completely prevent heart failure (HF) from proceeding to an advanced stage. Cardiac transplantation is the last choice to save the patient at the end stage, and this treatment entails many sociomedical problems. An alternative strategy for therapy is urgently required (1, 2). Primary or secondary degradation of dystrophin (Dys) might be of great significance in determining the cause of HF. Muscular dystrophy results in HF, and poor outcome in patients and animal models is associated with genetic mutations of Dys or the sarcoglycan (SG) complex (1–6). In the present study, we examined the following phenomena: (*i*) the time course of the hemodynamics with biventricular catheterization under stable anesthesia (7) until the TO-2 animals started to show overt HF and cardiac death; (*ii*) *in situ* sarcolemma (SL) stability by double fluoromicroscopy for the entry of an SL-impermeable dye, Evans blue dye (EB), into cardiomyocytes (8) and immunostaining of Dys or δ-SG; (*iii*) Western blotting of Dys and protein quantification; (*iv*) the correlation between limited proteolysis of Dys and hemodynamics; and (*v*) *in vivo* gene transduction in TO-2 hamsters. We also evaluated pathological features in rats with acute and acquired HF due to isoproterenol (Isp) toxicity (9) and in humans with advanced dilated cardiomyopathy (DCM).

Materials and Methods

Experimental Animals, the *rAAV* Vector Gene Construct, and *in Vivo* Gene Delivery. Male F_1B (control) and TO-2 hamster strains were obtained from Bio Breeders (Watertown, MA), and rAAV/lacZ vector alone or a mixture of recombinant adenoassociated virus (rAAV)/lacZ and rAAV/δ-SG was intramurally injected into the cardiac apex of the 5-week-old hamsters (7). pW1, an rAAV plasmid containing lacZ or a 1.2-kb fragment of δ-SG cDNA flanked by inverted terminal repeats of the AAV genome, pHLP19, a helper plasmid with *rep* and *cap* genes, and pladeno-1, a plasmid harboring the adenovirus *E2A*, *E4*, and *VA* genes, were used for rAAV/lacZ or rAAV/δ-SG production. pWSG with a δ-SG expression cassette driven by a cytomegalovirus (CMV) promoter was used for rAAV/δ-SG production (7, 8). Under open chest surgery with constant-volume ventilation, rAAV/lacZ alone or a mixture of rAAV/lacZ and rAAV/δ-SG was intramurally injected into the cardiac apex twice (each injection was 15 μl, for a total of 8.4×10^{10} and 6×10^{10} copies for lacZ and δ-SG, respectively).

Morphological and Immunological Analyses. A polyclonal, site-directed antibody to δ-SG was prepared at a high titer, by using a synthetic peptide with a sequence deduced from the cloned cDNA as a specific epitope (4). Monoclonal antibodies to Dys and to the transgene of lacZ (β-galactosidase) were obtained from NovoCastra (Newcastle, U.K.) and Funakoshi (Tokyo). The density of antibody-specific bands for the rod domain of Dys was measured within a linear intensity range for the applied amount of protein, after Western blotting of whole-heart homogenates, by 5–15% SDS/PAGE. For the Isp study, 10–20% SDS/PAGE was used to detect degradation products of both Dys and δ-SG. To simultaneously monitor Dys disruption, SL fragility *in situ*, and expression of the δ-SG transgene, double fluoromicroscopy was used to detect immunostaining of Dys with a FITC-labeled antibody specific to the rod domain of Dys, the entry of membrane-impermeable EB into cardiomyocytes, and immunostaining of δ-SG with a rhodium isothiocyanate (RITC)-labeled specific antibody by using a Nikon Diaphot or a Leica (Heidelberg, Germany) TCS SL confocal microscope. Where indicated, the Dys immunoproduct in the SL and myoplasm was semiquantified on cardiomyocytes, with or without transduction of δ-SG in the same observation field.

Abbreviations: HF, heart failure; Dys, dystrophin; SG, sarcoglycan; SL, sarcolemma; EB, Evans blue dye; Isp, isoproterenol; DCM, dilated cardiomyopathy; rAAV, recombinant adenoassociated virus; LVP, left ventricular pressure; EDP, end diastolic pressure; CVP, central venous pressure.

§To whom correspondence should be addressed. E-mail: toyooka.3im@hotmail.com.

Table 1. Cardiac hemodynamics with progression of HF

Strain	Age, weeks	LVP, mmHg	dP/dt_{max}, mmHg/sec	dP/dt_{min}, mmHg/sec	EDP, mmHg	CVP, mmHg
F_1B	5	82.9 ± 1.2	4,385 ± 91	−4,503 ± 208	3.1 ± 0.6	1.70 ± 0.53
	15	132.9 ± 5.5†	8,188 ± 743†	−7,188 ± 971†	1.8 ± 1.5	0.78 ± 0.50
	25	132.5 ± 6.9	6,709 ± 188	−6,513 ± 602	1.7 ± 2.7	0.46 ± 0.21
	40	125.1 ± 9.6	7,063 ± 290	−7,180 ± 576	1.6 ± 0.9	−0.62 ± 0.32
TO-2	5	83.0 ± 2.1	4,599 ± 192	−5,175 ± 233*	1.9 ± 0.3*	2.82 ± 0.17*
	15	100.2 ± 4.7*†	4,645 ± 637*	−3,664 ± 378*†	8.8 ± 1.9*†	2.70 ± 0.87*
	25	87.9 ± 8.3*	5,240 ± 388*	−3,171 ± 80*	12.8 ± 1.6*	3.12 ± 0.88*
	40	80.0 ± 2.8*	4,283 ± 97*	−3,120 ± 145*	18.0 ± 1.4*†	9.35 ± 1.35*†

Hemodynamic indices measured under stable anesthesia (7, 8): LVP, its maximum derivative (dP/dt_{max}) and minimum derivative (dP/dt_{min}), EDP, and CVP, in control (F_1B strain) and hereditary DCM (TO-2 strain) hamsters. Each value is shown as the mean ± SE (n = 4–8 hamsters in each group). * and † indicate statistical significance ($P < 0.05$) compared with the F_1B strain and the preceding age, respectively.

Hemodynamic Studies and Statistical Analyses. Peak left ventricular pressure (LVP), left ventricular end diastolic pressure (EDP), its first derivative (dP/dt), and central venous pressure (CVP) were measured under stable anesthesia (7, 8). All values were expressed as the mean ± SE and evaluated by paired Student's t test, ANOVA, and correlation analyses. A P value of <0.05 was considered significant.

Results and Discussion

Progression of DCM to Advanced HF in TO-2 Hamsters. Control F_1B hamsters showed growth-dependent increases in the peak LVP, the maximum rate of LVP (dP/dt_{max}), and the minimum rate of LVP (dP/dt_{min}, Table 1). In contrast, TO-2 hamsters persistently demonstrated systolic failure characterized by reduced LVP, dP/dt_{max}, and blunted dP/dt_{min}. Congestive HF was documented by increased left ventricular EDP and CVP. These signs became aggravated between 25 and 40 weeks of age, when the rate of cardiac death sharply increased (see below). The EDP and CVP reached levels 9.5 and 3.3 times higher, respectively, than those at 5 weeks of age.

Translocation of Dys from the SL to the Myoplasm During DCM Progression. Cardiac samples from TO-2 hamsters revealed time-dependent pathological features at each age (Fig. 1). After 5 weeks, double fluoromicroscopy showed that Dys was neatly arranged on the SL, and EB administered *i.v.* before killing the animals did not enter the myoplasm, indicating that the integrity of the SL was well preserved. After 25 and 40 weeks, the Dys on the SL became blurred, and some cardiomyocytes demonstrated a shift of Dys from the SL to the myoplasm. We refer to this phenomenon as "translocation" of Dys. These cardiomyocytes matched exactly with cells that took up EB (within ovals), denoting that the SL of the translocated cells leaked the exogenously applied dye.

Cleavage of Dys in Hamster Heart and in the Hearts of Humans with DCM. Western blotting of the myocardial homogenate with an antibody specific to the rod domain of Dys showed characteristic features (Fig. 2*a Left*). Normal hearts at 5 weeks of age showed a band at 430 kDa corresponding to normal Dys, and the staining intensity was preserved up to 40 weeks of age. Striking differences were observed in TO-2 hamsters, although at 5 and 15 weeks of age the staining pattern did not differ from that of the F_1B heart. However, at 25 weeks of age, extra bands were detected between 60 and 200 kDa (Fig. 2*a Left*), and the intensity of the Dys 430-kDa band started to decline. The intensity of this band was markedly reduced between 25 and 40 weeks of age, whereas the intensity of the 60-kDa band increased, mirroring the Dys band (Fig. 2*b*). The period of significant Dys cleavage matched exactly the periods when Dys translocation became

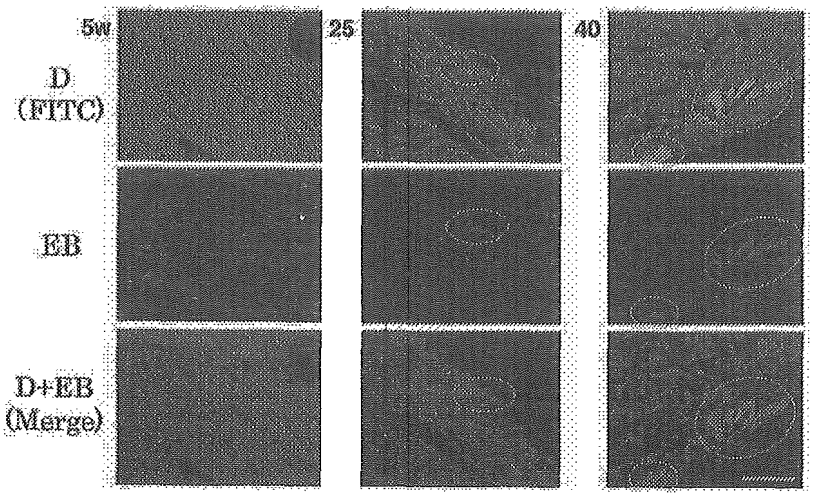

Fig. 1. Age-dependent translocation of Dys and increased permeability of the SL during HF progression in TO-2 hamsters. Double fluoromicroscopy for detection of a FITC-labeled antibody to the rod domain of Dys and entry of membrane-impermeable, fluorescent EB, at 5, 25, and 40 weeks of age (w). Cardiomyocytes demonstrating a shift of Dys from the SL to the myoplasm are shown in ovals. (Bar = 40 μm.)

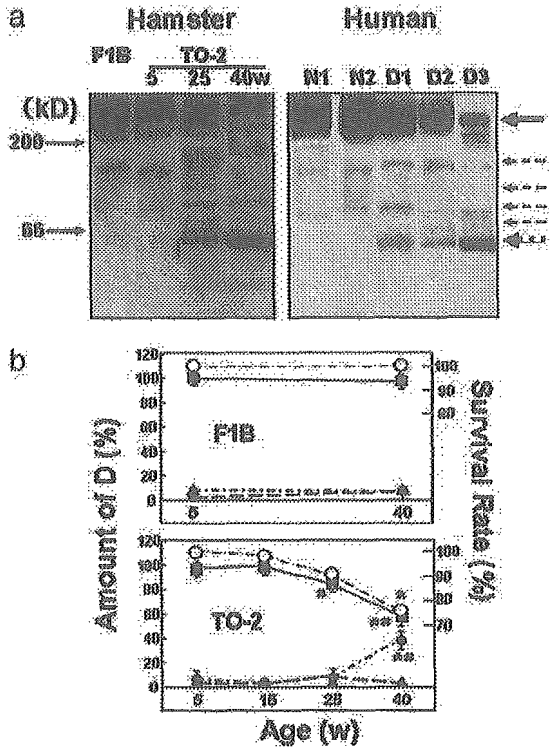

Fig. 2. Cleavage and reduction of cardiac Dys during DCM progression in hamsters and humans. (*a Left*) Control (F_1B strain) or DCM (TO-2 strain) hamsters at 5, 25, and 40 weeks of age (w). (*a Right*) Normal human myocardium (N1 and N2) and DCM hearts (D1, D2, and D3) at the time of cardiac transplantation. A solid arrow at 430 kDa and several dotted arrows denote the original Dys and its degradation products, respectively, after 5–20% SDS/PAGE of whole-heart homogenates. (*b*) Time course of the survival rate of control (F_1B; *Upper*) or DCM (TO-2; *Lower*) hamsters (○) and the density of immunoreactive bands specific to the rod domain of Dys at 430 (▩), 60 (●) or 160 (▲) kDa. * and # indicate a significant difference, compared with the control F_1B strain and the preceding age, respectively.

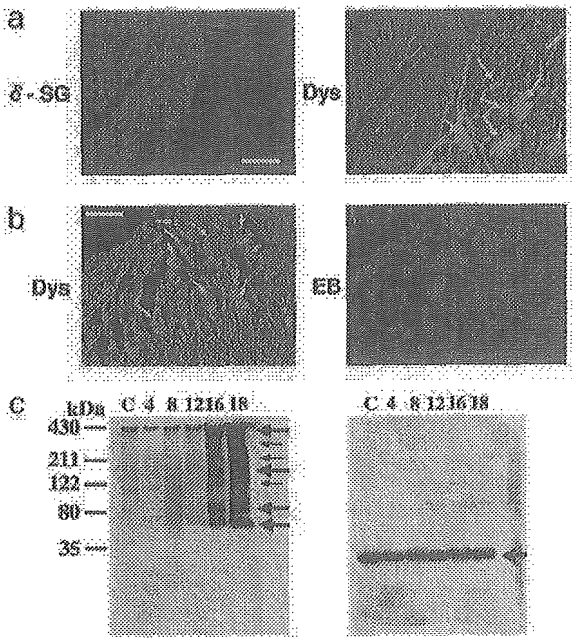

Fig. 3. (a) Double immunostaining of δ-SG (rhodamine isothiocyanate) and Dys (FITC) of TO-2 hamster hearts 35 weeks after local δ-SG gene transfection *in vivo* (8). Arrows indicate cardiomyocytes where dystrophin was translocated from the SL to the myoplasm. (Bar = 40 μm.) (*b*) Assessment of Dys translocation (FITC) and SL fragility *in situ* (EB entry) 16 h after the administration of Isp at a high dose (10 mg/kg i.p.) in Wistar rats (15). Arrows indicate cardiomyocytes where dystrophin was translocated from the SL to the myoplasm. (Bar = 40 μm.) (*c*) Western blotting of Dys (*Left*) and δ-SG (*Right*) from the same rat heart homogenate sample after gradient 10–15% SDS/PAGE of the control (C) and 4, 8, 12, 16 and 18 h after Isp treatment. Arrows indicate uncleaved Dys (430 kDa) and Dys degradation products (*Left*) or δ-SG (*Right*).

evident (Fig. 1) and when the animals started to die of congestive HF (ref. 8 and Fig. 2*b*). The intensity of the faint 160-kDa band did not change throughout the study and appeared to be unrelated to the progression of HF.

Similar cleavage of Dys was confirmed in hearts from patients with DCM of unidentified etiology who had undergone cardiac transplantation (Fig. 2*a Right*). The topological shift of Dys was also documented in samples of advanced stage DCM (unpublished data). Accordingly, the translocation was common to both animal models and patients with DCM. Other antibodies to the C or N terminus of Dys did not clearly recognize the cleavage product (data not shown). At present, we do not know the reason for this discrepancy in human cases of advanced HF showing selective cleavage of Dys at the N terminus (10).

Relationship of Dys Cleavage to Hemodynamics and the Lifespan of Hamsters. Surprisingly, the amount of Dys or its 60-kDa-band degradation product in TO-2 animals very closely correlated with the hemodynamic indices that characterize the progression of HF. The Dys amount was positively correlated with the systolic index [peak LVP, coefficient of regression (r) = 0.998 and $P < 0.0004$], and negatively correlated with the diastolic parameters (EDP, $r = 0.996$ and $P < 0.0005$; CVP, $r = 0.954$ and $P < 0.002$). The intensity of the 60-kDa band showed a clear negative correlation with the LVP ($r = 0.961$, $P < 0.002$) and a positive correlation with the EDP ($r = 0.954$, $P < 0.002$) and CVP ($r = 0.996$, $P < 0.0005$). These highly significant regression coefficients for correlation of the amount of Dys with systolic or diastolic performance support a tentative role for Dys in transmitting an effect through the actin–myosin linkage to the extracellular matrix. It is also noteworthy that no correlation was found between the amounts of Dys or the 60-kDa band and the dP/dt_{max} or dP/dt_{min} value (data not shown), both of which are regulated by Ca^{2+} handling (11) and the energetics of cardiac muscle cells (12). It should be emphasized that a distinct relationship was found between the amount of Dys or the 60-kDa band and the survival rate of the TO-2 animals over time (Fig. 2*b Lower*). It is possible that these immunological and hemodynamic data could be biased, because ≈30% of the TO-2 hamsters died of HF (Fig. 2*b Lower*), and we could only use the survivors in the analysis.

Effect of Long-Lasting Gene Therapy on Dys Localization. The final evidence that the disruption of Dys is not an epiphenomenon in HF but is actually caused by a loss of δ-SG is provided by the double immunostaining of Dys and δ-SG in TO-2 hearts with or without local gene transfection *in vivo* (Fig. 3*a*). In control F_1B hearts, both proteins were equally expressed on the SL (data not shown). In contrast, the TO-2 heart did not express δ-SG (13). As described above (Fig. 1), Dys staining became blurred with age, and some cardiomyocytes revealed Dys translocation (14). Gene delivery of normal δ-SG *in vivo*, by means of a nonpathogenic and long-lasting rAAV vector (7, 8), was used to locally express the δ-SG transgene, and this gene therapy completely ameliorated Dys translocation in the same cardiomyocytes for up to 35 weeks (Fig. 3*a Left*). In contrast, nontransfected cells

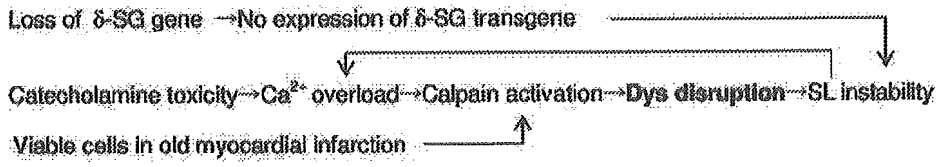

Scheme 1. Pathways for the progression of HF to an advanced stage.

showed translocation of Dys in the same sample (indicated by arrows in Fig. 3*a Right*). This finding specifically eliminates the possibility that Dys disruption resulted from the parallel development of HF, because Dys translocation was restricted to cardiomyocytes that did not express the δ-SG transgene. Furthermore, the amount of Dys estimated *in situ* by densitometry of immunofluoromicroscopic images in cardiomyocytes indicated a 1.22 ± 0.13 fold ($P < 0.01$) preferential localization of Dys on the SL of δ-SG-transfected cells ($n = 70$ cells per group).

Effect of Isp on SL Permeability, and Shift and Cleavage of Dys and δ-SG. A toxic dose of Isp (10 mg/kg i.p.) causes acute HF and morphological deterioration in normal rats (9). Pathological examination has shown time-dependent degradation of Dys and apoptosis of cardiomyocytes from 4 to 18 h after Isp was administered (15). Confocal microscopy of cardiomyocytes in the same observation field showed translocation of Dys (indicated by arrows in Fig. 3*b Left*) and entry of the SL-impermeable EB into the myoplasm of cardiac muscle cells. The shift of Dys was selectively detected 16 h after Isp treatment only in cardiomyocytes where EB had entered the myoplasm (Fig. 3*b Right*). Western blotting revealed time-dependent cleavage of Dys, showing degradation fragments between 60 and 200 kDa (Fig. 3*c Left*). In contrast, δ-SG was not hydrolyzed at all (Fig. 3*c Right*). Immunohistology confirmed that δ-SG did not shift from the SL but remained localized on the SL (data not shown). The effect of high-dose Isp, a β-adrenergic agonist, was similar to that observed in a DCM mouse with a protein kinase A knock-in gene (16). To verify the therapeutic effect of gene therapy in a β-adrenergic agonist/protein kinase A/phospholamban system, the pharmacological action (17, 18) and the disease prognosis need to be precisely examined, because an improvement in hemodynamics does not always prolong the lifespan of the animal (19).

The limited hydrolysis of Dys, common to the models of acute and chronic diseases in the present study, suggests a role for calpain, because cardiomyocytes contain an appreciable amount of this protein (20), and intracellular Ca^{2+} handling is modified in failing hearts (21, 22). Neither a specific inhibitor for calpain nor a calpain knockout animal is currently available to test this hypothesis. β-Adrenergic agonists induce Ca^{2+} overload in cardiomyocytes by increasing Ca^{2+} uptake (23). In addition, Dys and α-, β-, and γ-SG, but not δ-SG, are hydrolyzed by the endogenous protease (24) or isolated calpain *in vitro* (25, 26). The preferential breakdown of these proteins, but not δ-SG, in three HF models, i.e., TO-2 hamster hearts (13), Isp-treated rat hearts (Fig. 3*b*), and viable cells at the end stage of myocardial infarction (26), might be accompanied by substantially enhanced activity of *m*-calpain over its endogenous inhibitor, calpastatin. The expression of *m*-calpain in TO-2 hearts markedly exceeded that of calpastatin during the progression of HF (data not shown). These results may imply that the balance between calpain and calpastatin will shift in a calpain-dominant manner. Furthermore, dot hybridization analyses revealed no increment of mRNA of each DAP component under these HF conditions, suggesting that compensatory biosynthesis did not occur in the case of DAP.

A Scheme for the Progression of HF to an Advanced Stage. The clinical link between excess stimulation with catecholamines and myocardial damage has been confirmed by the therapeutic success of β-adrenergic antagonists in TO-2 hamsters (27) and humans (28, 29). The cleavage of Dys has also been documented after enterovirus infection, resulting in DCM-like HF (30). These pathological findings present a paradigm in which cardioselective cleavage of Dys may lead to progression of HF to an advanced stage (Scheme 1). Scheme 1 does not exclude the involvement of a protease cascade, as seen through the activation of a calpain-like homologue in neuronal degeneration in *Caenorhabditis elegans* (31), or involvement of the ubiquitin/proteasome system (32) in the loss of Dys. More definite evidence is required to precisely determine the causative factor(s). This common pathological process, irrespective of the hereditary or acquired origin and the chronic or acute course of the disease, suggests a strategy for the treatment of advanced HF through interruption of the vicious circle by either gene therapy or drug treatment.

We thank Dr. John R. Solaro (Department of Physiology and Biophysics, University of Illinois, Chicago) for discussion of the results and Dr. Y. Niwa and K. Kurosawa (Department of Pathophysiology, University of Tokyo) for experimental and secretarial assistance. This work was supported by Ministry of Education, Culture, and Science Grant A2 142070333 and by the Ministry of Welfare and Labor, Japan, the Mitsubishi Research Foundation, and the Motor Vehicle Foundation.

1. Cox, G. F. & Kunkel, L. M. (1997) *Curr. Opin. Cardiol.* **12**, 329–343.
2. Seidman, J. G. & Seidman, C. (2001) *Cell* **104**, 557–567.
3. Durbeej, M. & Campbell, K. P. (2002) *Curr. Opin. Genet. Dev.* **12**, 349–361.
4. Sakamoto, A., Ono, K., Abe, M., Jasmin, G., Eki, T., Murakami, Y., Masaki, T., Toyo-oka, T. & Hanaoka, F. (1997) *Proc. Natl. Acad. Sci. USA* **94**, 13873–13878.
5. Nigro, V., Okazaki, Y., Belsito, A., Piluso, G., Matsuda, Y., Politano, L., Nigro, G., Ventura, C., Abbondanza, C., Molinari, A. M., *et al.* (1997) *Hum. Mol. Genet.* **6**, 601–607.
6. Tsubata, S., Bowles, K. R., Vatta, M., Zintz, C., Titus, J., Muhonen, L., Bowles, N. E. & Towbin, J. A. (2000) *J. Clin. Invest.* **106**, 655–662.
7. Kawada, T., Sakamoto, A., Nakazawa, M., Urabe, M., Masuda, F., Hemmi, C., Wang, Y., Shin, W. S., Nakatsuru, Y., Sato, H., *et al.* (2001) *Biochem. Biophys. Res. Commun.* **284**, 431–435.
8. Kawada, T., Nakazawa, M., Nakauchi, S., Yamazaki, K., Shimamoto, R., Urabe, M., Nakata, J., Masui, F., Nakajima, T., Suzuki, J., *et al.* (2002) *Proc. Natl. Acad. Sci. USA* **99**, 901–906.
9. Kahn, D. S., Rona, G. & Chappel, C. I. (1969) *Ann. N.Y. Acad. Sci.* **156**, 285–293.
10. Vatta, M., Stetson, S. J., Perez-Verdia, A., Entman, M. L., Noon, G. P., Torre-Amione, G., Bowles, N. E. & Towbin, J. A. (2002) *Lancet* **359**, 936–941.
11. Ebashi, S., Nonomura, Y., Toyo-oka, T. & Katayama, E. (1976) *Symp. Soc. Exp. Biol.* **30**, 349–360.
12. Toyo-oka, T., Nagayama, K., Suzuki, J. & Sugimoto, T. (1992) *Circulation* **86**, 295–301.
13. Kawada, T., Nakatsuru, Y., Sakamoto, A., Koizumi, T., Shin, W. S., Okai-Matsuo, Y., Suzuki, J., Uehara, Y., Nakazawa, M., Satoh, H., *et al.* (1999) *FEBS Lett.* **458**, 405–408.
14. Kawada, T., Hemmi, C., Fukuda, S., Iwasawa, K., Tezuka, A., Nakazawa, M., Sato, H. & Toyo-oka, T. (2004) *Exp. Clin. Cardiol.* **8**, in press.
15. Xi, H., Shin, W. S., Suzuki, J., Nakajima, T., Kawada, T., Uehara, Y., Nakazawa, M. & Toyo-oka, T. (2000) *J. Cardiovasc. Pharmacol.* **36**, Suppl. 2, S25–S29.
16. Antos, C. L., Frey, N., Marx, S. O., Reiken, S., Gaburjakova, M., Richardson, J. A., Marks, A. R. & Olson, E. N. (2001) *Circ. Res.* **89**, 997–1004.

17. Bristow, M. R. (2001) *Circulation* **103,** 787–788.
18. Hoshijima, M., Ikeda, Y., Iwanaga, Y., Minamisawa, S., Date, M. O., Gu, Y., Iwatate, M., Li, M., Wang, L., Wilson, J. M., *et al.* (2002) *Nat. Med.* **8,** 864–871.
19. Jessup, M. & Brozena, S. (2003) *N. Engl. J. Med.* **348,** 2007–2018.
20. Toyo-oka, T., Shimizu, T. & Masaki, T. (1978) *Biochem. Biophys. Res. Commun.* **82,** 484–491.
21. Gwathmey, J. K., Copelas, L., MacKinnon, R., Schoen, F. J., Feldman, M. D., Grossman, W. & Morgan, J. P. (1987) *Circ. Res.* **61,** 70–76.
22. Whitmer, J. T., Kumar, P. & Solaro, R. J. (1988) *Circ. Res.* **62,** 81–85.
23. Naylor, W. G., Mas-Oliva, J. & Williams, A. J. (1980) *Circ. Res.* **46,** Part 2, 161–166.
24. Koenig, M. & Kunkel, L. M. (1990) *J. Biol. Chem.* **265,** 4560–4566.
25. Yoshida, M., Suzuki, A., Shimizu, T. & Ozawa, E. (1992) *J. Biochem.* **112,** 433–439.
26. Yoshida, H., Takahashi, M., Koshimizu, M., Tanonaka, K., Oikawa, R., Toyo-oka, T. & Takeo, S. (2003) *Cardiovasc. Res.* **59,** 419–427.
27. Opie, L. H., Walpoth, B. & Barsacchi, R. (1985) *J. Mol. Cell. Cardiol.* **17,** Suppl. 2, 21–34.
28. Gottlieb, S. S., McCarter, R. J. & Vogel, R. A. (1998) *N. Engl. J. Med.* **339,** 489–497.
29. Packer, M., Coats, A. J., Fowler, M. B., Katus, H. A., Krum, H., Mohacsi, P., Rouleau, J. L., Tendera, M., Castaigne, A., Roecker, E. B., *et al.* (2001) *N. Engl. J. Med.* **344,** 1651–1658.
30. Badorff, C., Lee, G. H., Lamphear, B. J., Martone, M. E., Campbell, K. P., Rhoads, R. E. & Knowlton, K. U. (1999) *Nat. Med.* **5,** 320–326.
31. Syntichaki, P., Xu, K., Driscoll, M. & Tavernarakis, N. (2002) *Nature* **419,** 939–944.
32. Bonuccelli, G., Sotgia, F., Schubert, W., Park, D. S., Frank, P. G., Woodman, S. E., Insabato, L., Cammer, M., Minetti, C. & Lisanti, M. P. (2003) *Am. J. Pathol.* **163,** 1663–1675.

Available online at www.sciencedirect.com
SCIENCE DIRECT®
Biochemical and Biophysical Research Communications 319 (2004) 50–57
BBRC
www.elsevier.com/locate/ybbrc

RNAi induction and activation in mammalian muscle cells where *Dicer* and *eIF2C* translation initiation factors are barely expressed

Noriko Sago,[a,b,1] Kazuya Omi,[a,b,1] Yoshiko Tamura,[a] Hiroshi Kunugi,[a] Teruhiko Toyo-oka,[c] Katsushi Tokunaga,[b] and Hirohiko Hohjoh[a,*]

[a] *National Institute of Neuroscience, NCNP, 4-1-1 Ogawahigashi, Kodaira, Tokyo 187-8502, Japan*
[b] *Department of Human Genetics, Graduate School of Medicine, The University of Tokyo, 7-3-1 Hongo, Bunkyo-ku, Tokyo 113-0033, Japan*
[c] *Department of Pathophysiology and Internal Medicine, The University of Tokyo, 7-3-1 Hongo, Bunkyo-ku, Tokyo 113-0033, Japan*

Received 25 February 2004
Available online 10 May 2004

Abstract

Dicer plays an important role in the course of RNA interference (RNAi), i.e., it digests long double-stranded RNAs into 21–25 nucleotide small-interfering RNA (siRNA) duplexes functioning as sequence-specific RNAi mediators. In this study, we investigated the expression levels of *Dicer* and *eIF2C1~4*, which, like *Dicer*, appear to participate in mammalian RNAi, in various mouse tissues. Results indicate that the levels of *eIF2C1~4* as well as *Dicer* are lower in skeletal muscle and heart than in other tissues. To see if RNAi could occur under such a condition with low levels of expression of *Dicer* and *eIF2C1~4*, we examined RNAi activity in mouse skeletal muscle fibers. The results indicate that RNAi can be induced by synthetic siRNA duplexes in muscle fibers. We further examined RNAi activity during myogenic differentiation of mouse C2C12 cells. The data indicate that although the expression levels of *Dicer* and *eIF2C1~4* decrease during the differentiation, RNAi can be induced in the cells. Altogether, the data presented here suggest that muscle cells retain the ability to induce RNAi, although *Dicer* and *eIF2C1~4* appear to be barely expressed in them.

Keywords: RNA interference; Dicer; eIF2C translation initiation factors; Muscle; C2C12 cell

RNA interference (RNAi) is the process of a sequence-specific post-transcriptional gene silencing triggered by double-stranded RNAs (dsRNAs) homologous to the silenced genes. This intriguing gene silencing has been found in various species including flies, worms, protozoa, vertebrates, and higher plants (reviewed in [1–4]). DsRNAs introduced or generated in cells are digested by an RNase III enzyme, Dicer, into 21–25 nucleotide (nt) RNA duplexes [5–8] and the resultant duplexes, referred to as small-interfering RNA (siRNA) duplexes, function as essential sequence-specific RNAi mediators in the RNA-induced silencing complexes (RISCs) [5,7]. Thus, Dicer appears to play an important role in the process of RNAi induction.

In mammalian cells except for a part of undifferentiated cells [9–12], long dsRNAs (>30 bp) can trigger a rapid and non-specific RNA degradation involving the sequence-non-specific RNase, RNase L [13], and a rapid translation inhibition involving the interferon-inducible, dsRNA-activated protein kinase, PKR, instead of induction of RNAi [14]. In contrast, chemically synthesised siRNA duplexes can induce the sequence-specific RNAi activity in mammalian cells without triggering the rapid and non-specific RNA degradation and translation inhibition [15]. Together, it is likely that RNAi activity induced by the long dsRNAs could be masked by those rapid responses to the long dsRNAs in most of mammalian cells.

It may be of interest to examine the role of Dicer in differentiated mammalian cells possessing the rapid responses to long dsRNAs. Mammalian dicer has been identified and found to be a large multi-domain

* Corresponding author. Fax: +81-42-346-1744.
E-mail address: hohjohh@ncnp.go.jp (H. Hohjoh).
[1] These authors contributed equally to this work.

0006-291X/$ - see front matter © 2004 Elsevier Inc. All rights reserved.
doi:10.1016/j.bbrc.2004.04.151

polypeptide (~215 kDa) characterised by containing a putative DExH/DEAH RNA helicase/ATPase domain, a PAZ domain, two RNase domains, and a dsRNA-binding domain [16–20]. The expression of *Dicer* appears to be ubiquitous, but the level of its expression varies among tissues. Of the tissues examined previously, skeletal muscle appeared to express *Dicer* at a low level, i.e., the *Dicer* transcript appeared to be barely detectable at least using RT-PCR [16,17].

In this study, we investigated not only RNAi activity but also the expression levels of *Dicer* and *eIF2C1~4*, which, like *Dicer*, appear to participate in mammalian RNAi [21,22], in mouse skeletal muscle fibers, and muscle cells that differentiated from mouse C2C12 cells. The results indicate that RNAi can be induced by synthetic siRNA duplexes in those cells although the expression levels of *Dicer* and *eIF2C1~4* are lower than those in other tissues and undifferentiated C2C12 cells.

Materials and methods

Preparation and culture of muscle fibers isolated from extensor digitorum longus in mice. Isolation of muscle fibers from mice was carried out as described previously [23]. Briefly, extensor digitorum longus (EDL) was isolated from mice (ICR mouse strain), treated with 0.5% type 1 collagenase (Washington biochemical) in Dulbecco's modified Eagle's medium (DMEM) (Sigma), and incubated at 37 °C for 90 min. After incubation, the EDL was dissociated into single muscle fibers by gently pipetting, and dissociated single fibers were plated on matrigel-coated 24-well culture plates (approximately 100 fibers/well). The muscle fibers were cultured at 37 °C in DMEM supplemented with 10% horse serum (Invitrogen) in a 5% CO_2-humidified chamber. Two–three hours after starting culture, transfection was carried out.

Cell culture. C2C12 cells were grown at 37 °C in DMEM supplemented with 15% fetal calf serum (Sigma), 100 U/ml penicillin (Invitrogen), and 100 μg/ml streptomycin (Invitrogen) in a 5% CO_2-humidified chamber. For induction of myogenic differentiation, cells were cultured at 37 °C in DMEM supplemented with 5% horse serum (Invitrogen) in a 5% CO_2-humidified chamber [24]. The medium was changed everyday.

Synthetic oligonucleotides. RNA and DNA synthetic oligonucleotides were obtained from PROLIGO and SIGMAGENOSIS, respectively. The La2 siRNA duplex described previously was used in this study, and preparation of RNA duplexes was performed as described previously [25].

Transfection and luciferase assay. Reporter plasmids and siRNA duplexes were cotransfected into isolated single muscle fibers and undifferentiated and differentiated C2C12 cells using Lipofectamine 2000 (Invitrogen) according to the manufacturers' instructions. When undifferentiated C2C12 cells were used, the day before transfection, the cells were trypsinised, diluted with the fresh medium without

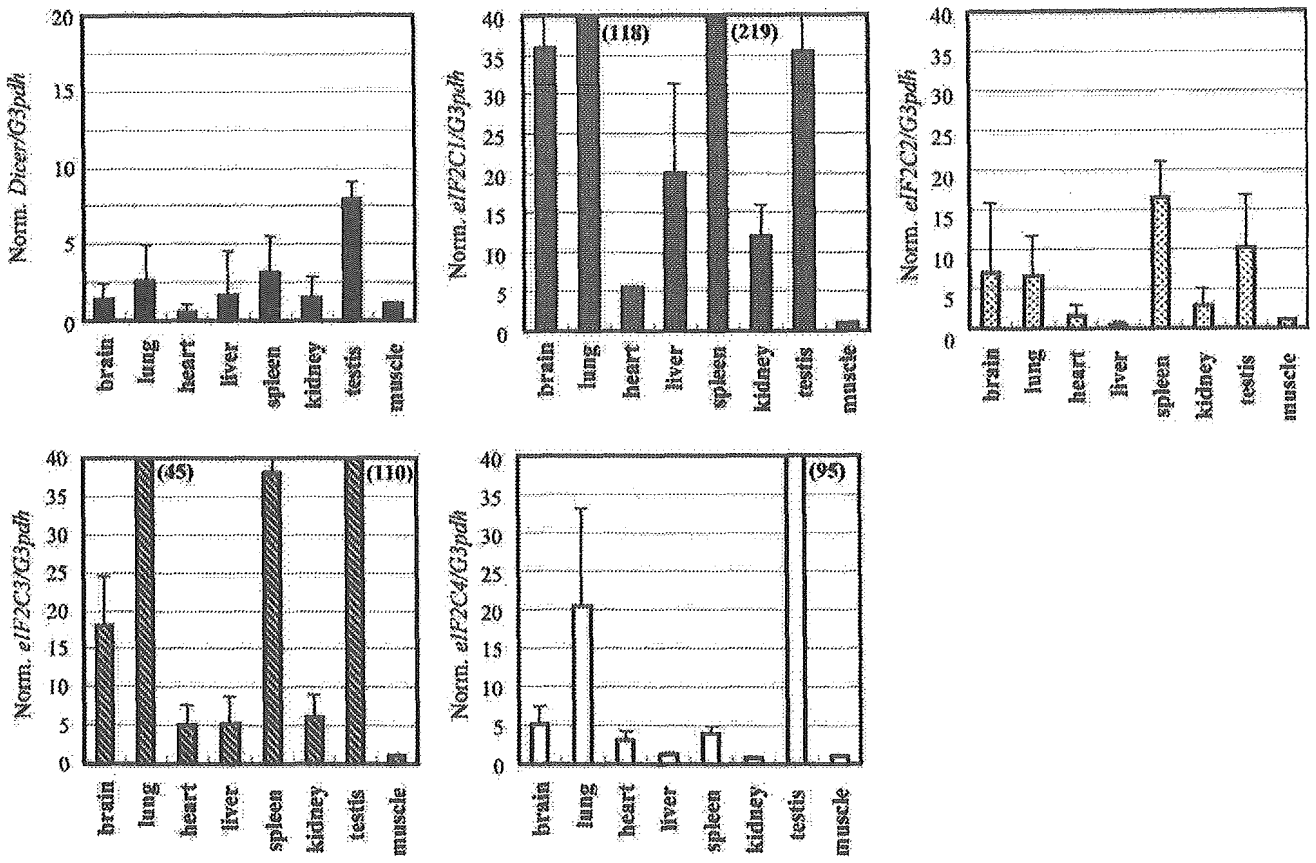

Fig. 1. Expression profiles of *Dicer* and *eIF2C1~4* in various mouse tissues. Total RNA was extracted from indicated tissues and subjected to cDNA synthesis with oligo(dT) primer and a reverse transcriptase. The expression levels of *Dicer* and *eIF2C1~4* were examined by means of a real-time PCR using the synthesised cDNAs as templates. The expression levels of the genes are normalised to that of the *G3pdh* gene examined as a control, and plotted when the expression level of either *Dicer* or *eIF2C1~4* in skeletal muscle is given as 1. Figures in parentheses indicate the averaged expression levels which are over the plotted areas. Data are averages of three independent experiments. Error bars represent standard deviations.

antibiotics, and seeded into 24-well culture plates (approximately 5×10^4 cells/well). Before the transfection, the culture medium was replaced with 0.5 ml OPTI-MEM I (Invitrogen), and to each well, 0.25 μg pGL3-control plasmid (Promega), 0.05 μg pRL-SV40 plasmid (Promega), and 0.2 μg siRNAs were applied. After 4-h incubation, 0.5 ml of the fresh culture medium without antibiotics was added, and further incubation at 37 °C was carried out. In the case of transfection into the isolated muscle fibers, the transfection mixture was directly applied into wells, and further incubation at 37 °C was carried out. When a short-hairpin expression plasmid, pRNA-U6.1/Neo/siRNA (GenScript), was used instead of synthetic siRNAs, 0.1 μg pGL3-control and 0.05 μg phRL-TK (Promega) together with various amounts of pRNA-U6.1/Neo/siRNA were introduced into C2C12 cells. The expression of luciferase was examined using a Dual-Luciferase reporter assay system (Promega) according to the directions provided by the manufacturer.

RT-PCR. Total RNA was extracted from the cultured cells and various mouse tissues using Trizol reagent (Invitrogen). Reverse-transcription (RT) for synthesizing the first-strand cDNAs was carried out using oligo(dT) primer and SuperScript II reverse transcriptase (Invitrogen) according to the manufacturer's instructions, and the resultant cDNAs were examined by real-time PCR using the ABI PRISM 7000 sequence detection system (Applied Biosystems) with a SYBER Green PCR Master Mix or a TaqMan Universal PCR Master Mix together with Assays-on-Demand Gene Expression products (Applied Biosystems) according to the manufacturer's instructions. For plotting a standard curve, the 1, 5, 25, 125, and 625-fold diluted brain cDNA samples, which were prepared from a brain tissue (total RNA) and designated as standards, were used in every real-time PCR. Expression levels of the genes examined were normalised to that of the control *G3pdh* gene. The PCR primers used in the real-time PCR were as follows:

G3pdh-F; 5′-TCTTCACCACCATGGAGAAG-3′
G3pdh-R; 5′-TCATGGATGACCTTGGCCAG-3′
Dicer-F; 5′-GCAGGCTTTTACACACGCCT-3′
Dicer-R; 5′-GGGTCTTCATAAAGGTGCTT-3′
eIF2C2-F; 5′-AGATGAAGAGGAAGTACCGT-3′
eIF2C2-R; 5′-CAGAACCAGCTTGTGCCTGT-3′

The Assays-on-Demand Gene Expression products used (the Assay ID numbers) were as follows:

eIF2C1; Mm00462977m1, *eIF2C3*; Mm00462959m1, *eIF2C4*; Mm00462659m1.

5-Bromodeoxyuridine incorporation assay. Cells were metabolically labeled in the culture medium containing 10 μM of 5-bromodeoxyuridine (BrdU) (Sigma) for 20 h, and rinsed with phosphate-buffered saline solution (PBS) followed by fixation with 70% ethanol containing 0.5 M HCl at −20 °C for 1 h. The resultant cells were incubated with anti-BrdU antibody (Oxford biotechnology) at 4 °C overnight. The BrdU-antibody complexes were visualised with Alexa488 conjugated secondary antibody (Invitrogen) and examined using a ZEISS (Axiovert) microscope.

Results and discussion

Expression profiles of Dicer and eIF2C1∼4 in various mouse tissues

Previous studies suggested that *Dicer* and *eIF2C* translation initiation factors (*eIF2C1∼4*) homologous to the *Ago* genes in *Drosophila* [26,27] contributed to mammalian RNAi [21,22]. *Dicer* appears to be expressed ubiquitously, but its expression level varies among tissues [16,17]. Since little is known about the expression levels of *eIF2C1∼4* among tissues, we first examined the levels of expression of *eIF2C1∼4* and *Dicer* in various tissues. Total RNA was extracted from mouse tissues and subjected to cDNA synthesis with oligo(dT) primer and reverse transcriptase. The resultant cDNAs were examined by a real-time PCR. The results are shown in Fig. 1. The expression level of *Dicer* in either skeletal muscle or heart appears to be lower than those in other tissues, which agrees with the previous observations [16,17]. It should be noted that the expression levels of *eIF2C1∼4* in either skeletal muscle or heart, like the expression profile of *Dicer*, are also significantly lower than those in the other tissues examined. Consequently, the observations suggest that

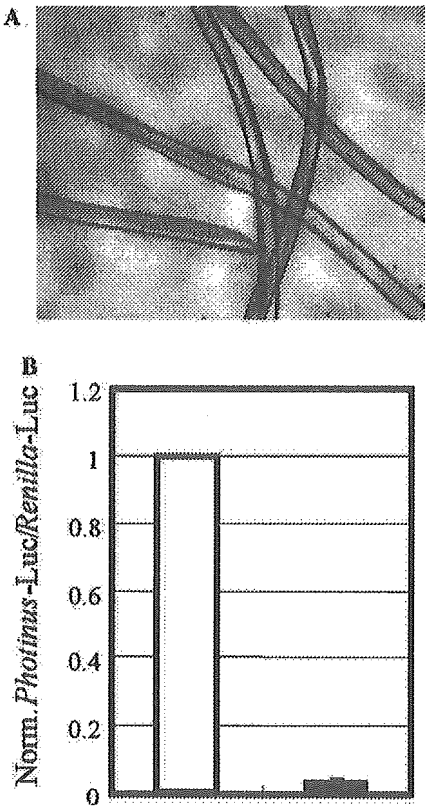

Fig. 2. RNAi induction by synthetic siRNA duplexes in muscle fibers prepared from mouse extensor digitorum longus. (A) Photograph of isolated muscle fibers. Isolation of muscle fibers from mouse extensor digitorum longus was carried out as described in Materials and methods. (B) RNAi activity in isolated muscle fibers. The La2 siRNA duplex against the *Photinus* luciferase gene [25] or a non-silencing siRNA duplex (Qiagen) together with pGL3-control and pRL-SV40 plasmids carrying *Photinus* and *Renilla* luciferase reporter genes, respectively, were cotransfected into the isolated muscle fibers. Twenty-four hours after transfection, cell lysate was prepared and dual luciferase assay was carried out. Ratios of normalised target (*Photinus*) luciferase activity to control (*Renilla*) luciferase activity are indicated: the ratios of luciferase activity determined in the presence of the La2 siRNA duplex are normalised to the ratios obtained in the presence of the non-silencing siRNA duplex. Open and solid bars indicate the data in the presence of the non-silencing siRNA and La2 siRNA duplexes, respectively. Data are averages of at least three independent experiments. Error bars represent standard deviations.

skeletal and cardiac muscle cells express either *Dicer* or *eIF2C1~4* at a low level.

RNAi activity in muscle fibers isolated from mouse extensor digitorum longus

The observations described above raised the question whether RNAi could occur in muscle, i.e., whether RNAi could be induced under a condition with a low level of expression of either *Dicer* or *eIF2C1~4*. In order to address the question, we isolated mouse muscle fibers from extensor digitorum longus of ICR mice (Fig. 2A), and introduced synthetic 21-nt siRNA duplex targeting the exogenous reporter gene, *Photinus* luciferase, together with a pGL3-control plasmid carrying the *Photinus luciferase* gene and a pRL-SV40 plasmid carrying the *Renilla luciferase* gene as a control into the isolated muscle fibers. For realizing an efficient RNAi induction, we used the La2 siRNA duplex having the potential for inducing a strong RNAi activity in cultured mammalian cells [25]. As shown in Fig. 2B, the results indicate that the La2 siRNA duplex can induce a strong gene silencing of the *Photinus luciferase* gene in the muscle fibers. This result suggests that RNAi can be induced by synthetic siRNA duplexes in skeletal muscle which barely expresses either *Dicer* or *eIF2C1~4*.

RNAi activity during myogenic differentiation of mouse C2C12 cells

To further examine the properties of RNAi in muscle cells and during myogenic differentiation, we investigated RNAi activity in C2C12 cells, a mouse myoblast cell line, which can be induced by changing culture conditions (detailed in Materials and methods) to differentiate into contractile myotubes [24]. First, we

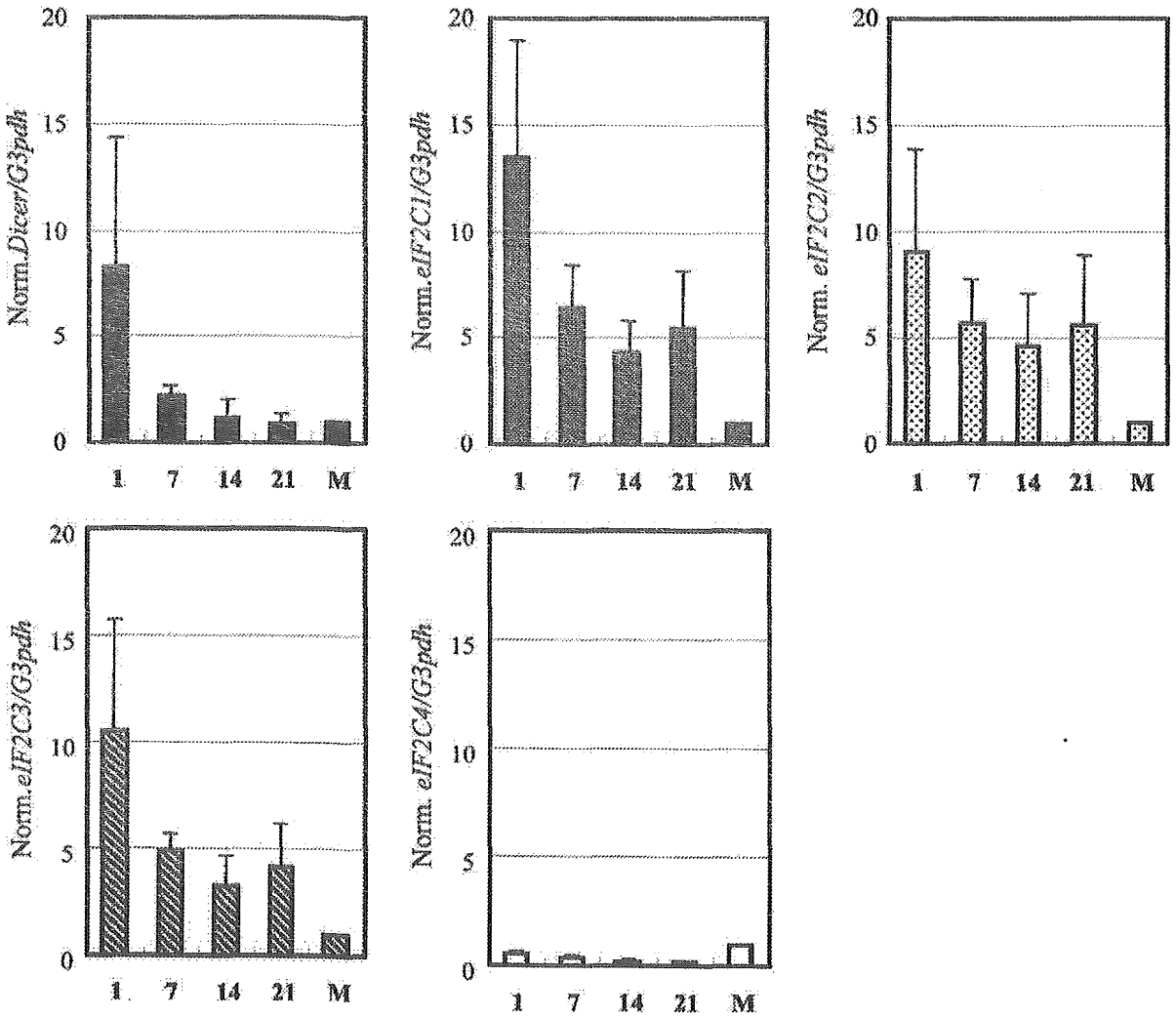

Fig. 3. Expression profiles of *Dicer* and *eIF2C1~4* during myogenic differentiation of mouse C2C12 cells. Total RNA was extracted from C2C12 cells at various days (indicated) after induction of myogenic differentiation of the cells (day 1 indicates undifferentiated C2C12 cells), and subjected to RT-PCR to examine the expression levels of *Dicer* and *eIF2C1~4* as in Fig. 1. The expression levels of the genes are normalised and plotted as in Fig. 1. M indicates skeletal muscle. Data are averages of three independent experiments. Error bars represent standard deviations.

examined the expression profiles of *Dicer* and *eIF2C1~4* during the myogenic differentiation of C2C12 cells and compared them with those of skeletal muscle examined above. As shown in Fig. 3, the expression profiles reveal that the level of expression of either *Dicer* or *eIF2C1~3* is gradually decreased during the myogenic differentiation of C2C12 cells, and that the *eIF2C4* gene is expressed at a low level in either C2C12 myoblast or myotube.

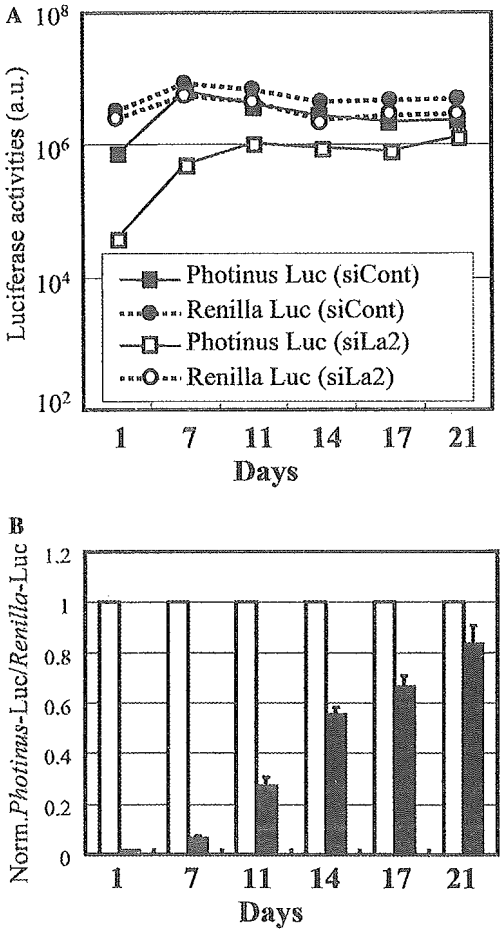

Fig. 4. Persistence of RNAi activity during myogenic differentiation of mouse C2C12 cells. The La2 siRNA duplex or a non-silencing siRNA duplex (Qiagen) together with pGL3-control and pRL-SV40 plasmids were cotransfected into C2C12 cells as in Fig. 2. Before transfection, the culture medium (DMEM containing 15% fetal calf serum) was replaced with DMEM containing 5% horse serum for induction of the myogenic differentiation of C2C12 cells. RNAi activity was examined 24 h after transfection (day 1), and thereafter examined at various days (indicated) up to 3 weeks after the transfection. (A) Absolute *Photinus* and *Renilla* luciferase expressions. The expression levels are plotted in arbitrary luminescence units (a.u.). (B) Ratios of normalised target to control luciferase. Ratios of normalised target (*Photinus*) luciferase activity to control (*Renilla*) luciferase activity are indicated as in Fig. 2. Open and solid bars indicate the data in the presence of the non-silencing siRNA and La2 siRNA duplexes, respectively. Data are averages of at least three independent experiments. Error bars represent standard deviations.

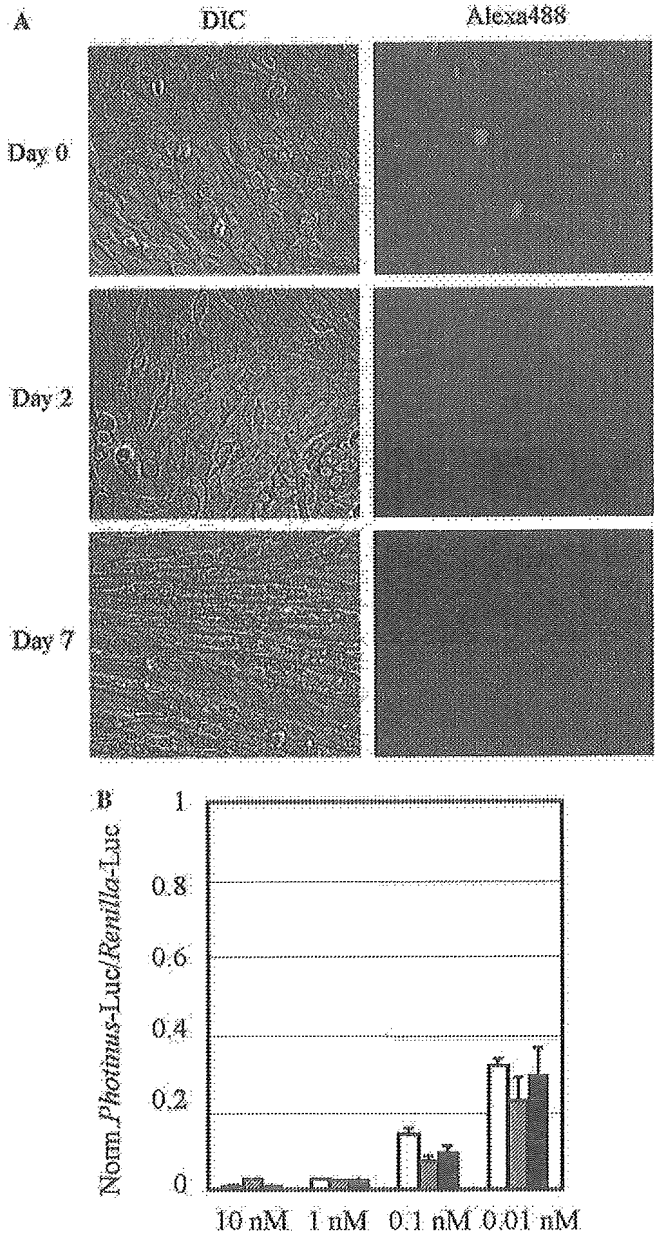

Fig. 5. Cell-cycle arrest and RNAi activity during myogenic differentiation of C2C12 cells. Myogenic differentiation of C2C12 cells was induced by changing the culture medium from DMEM containing 15% fetal calf serum to DMEM containing 5% horse serum. (A) Cell-cycle arrested C2C12 cells. Metabolically labeling of the cells with BrdU was carried out at indicated days after the differentiation. Day 0 indicates undifferentiated C2C12 cells. BrdU incorporated into the cells was visualised with an anti-BrdU antibody and an Alexa488 conjugated secondary antibody. The cells were examined by a florescent microscope. Left (DIC, differential interference contrast) and right (Alexa488, florescence image) panels are identical in visual field. (B) RNAi activity during the differentiation. The reporter plasmids carrying the *Photinus* and *Renilla luciferase* genes were cotransfected with a decreasing amount of the La2 siRNA or non-silencing siRNA duplexes (Qiagen), from 10 to 0.01 nM, into either undifferentiated or differentiated C2C12 cells. Ratios of normalised target (*Photinus*) luciferase activity to control (*Renilla*) luciferase activity are indicated as in Fig. 2. Open, dotted, and solid bars indicate the data in C2C12 cells that differentiated for 0 (undifferentiated), 2, and 7 days, respectively. Data are averages of at least three independent experiments. Error bars represent standard deviations.

Next we examined RNAi activity during the myogenic differentiation of C2C12 cells. The La2 siRNA duplex together with pGL3-control and pRL-SV40 plasmids was cotransfected into undifferentiated C2C12 cells, and simultaneously myogenic differentiation of the cells was carried out by changing culture medium as described above (see Materials and methods). As a result, a strong RNAi activity was detected by day 7 after RNAi induction (Fig. 4), when morphological changes of C2C12 cells into myotubes appeared to be completed (Fig. 5A); thereafter, the cells gradually lost the RNAi activity and lost most of the activity by day 21 after the induction (Fig. 4).

Because proliferating mammalian cells gradually lose RNAi activity with an increase in the number of cell divisions [12,28,29], we investigated whether cell division occurred in C2C12 cells during the differentiation by means of a BrdU incorporation assay. As shown in Fig. 5A, while the incorporation of BrdU into nuclei could be observed in undifferentiated C2C12 cells, few or no BrdU-positive cells were detectable at day 2 and 7 after induction of the differentiation. In addition, from the data of Fig. 5B, the nature of RNAi activity during the differentiation appears to remain unchanged. Consequently, these observations suggest that C2C12 cells differentiated over 2 days are probably cell-cycle arrested cells, and thus that the decrease in RNAi activity during the myogenic differentiation of C2C12 cells is not caused by cell division.

We further examined RNAi activities in C2C12 myotubes that differentiated for 14 and 21 days. The results indicate that RNAi activities induced by synthetic siRNA duplexes are detectable in those differentiated C2C12 myotubes (Fig. 6), although the transfection efficiency of siRNA and plasmid DNA into the cells seemed to become lower as the culture was long. Taking all the data together, it is conceivable that the decrease in RNAi activity during the myogenic

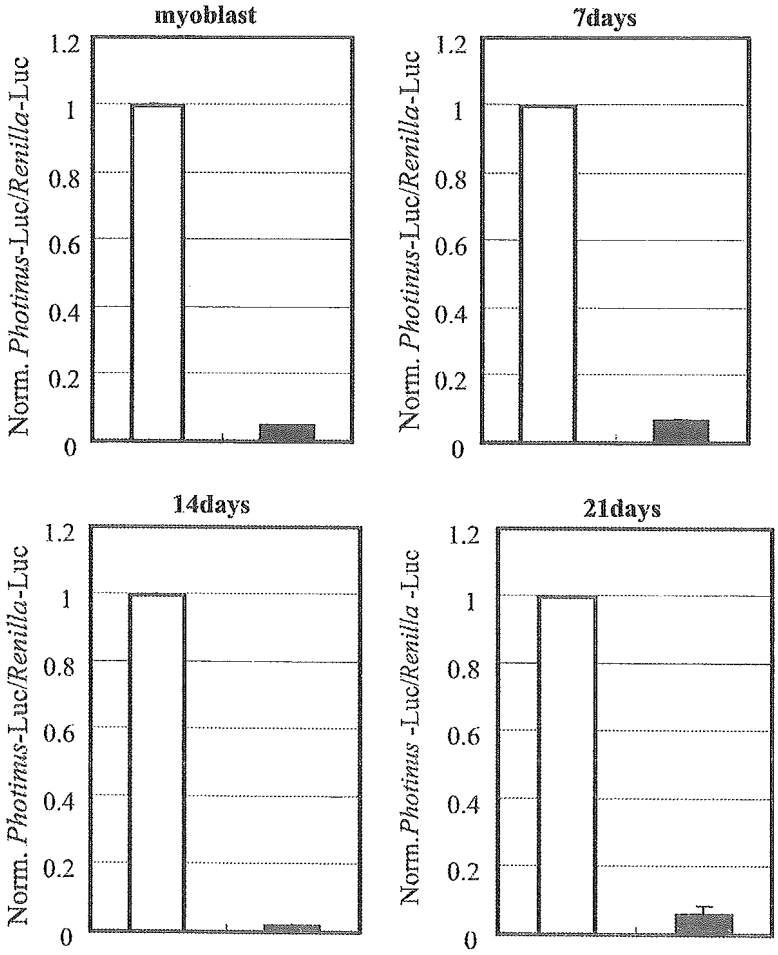

Fig. 6. RNAi induction after myogenic differentiation of C2C12 cells. Myogenic differentiation of C2C12 cells was performed as in Fig. 5. RNAi induction was carried out as in Fig. 2 at indicated days after induction of the myogenic differentiation, and each RNAi activity was examined 24 h after RNAi induction. Ratios of normalised target (*Photinus*) luciferase activity to control (*Renilla*) luciferase activity are indicated as in Fig. 2. Open and solid bars indicate the data in the presence of the non-silencing siRNA and La2 siRNA duplexes, respectively. Data are averages of at least three independent experiments. Error bars represent standard deviations.

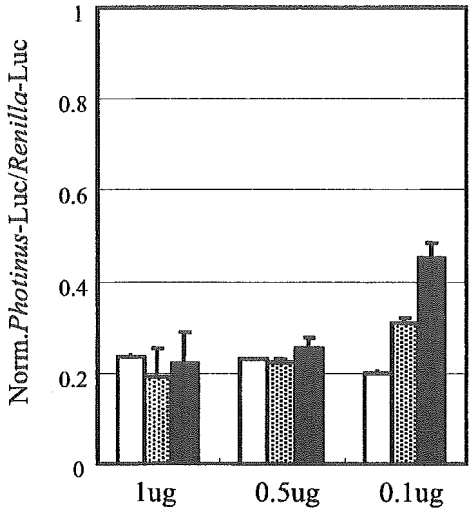

Fig. 7. RNAi induction by short-hairpin RNAs during myogenic differentiation of C2C12 cells. The pRNA-U6.1/Neo/siFluc plasmid (GenScript), which can express a short-hairpin RNA (shRNA) against *Photinus luciferase*, and pRNA-U6.1/Neo empty vector (GenScript) as a control were used. The pGL3-control and phRL-TK plasmids together with a decreasing amount of each of the pRNA-U6.1/Neo/siFluc and pRNA-U6.1/Neo (a negative control) plasmids, from 1 to 0.1 μg, were cotransfected into C2C12 cells. The expression of luciferase was examined 24 h after the transfection. Ratios of normalised target (*Photinus*) luciferase activity to control (*Renilla*) luciferase activity are indicated as in Fig. 2. Open, dotted, and solid bars indicate the data in C2C12 cells that differentiated for 0 (undifferentiated), 2, and 7 days, respectively. Data are averages of at least three independent experiments. Error bars represent standard deviations.

differentiation of C2C12 cell may be caused by losing the stability of functional RISCs in the differentiated C2C12 myotubes.

RNAi induction by short-hairpin RNAs in C2C12 cells

Because Dicer appears to be required for the process of short-hairpin RNAs (shRNAs) into siRNA duplexes, it may be of interest to see if shRNAs can induce RNAi in C2C12 myotubes which barely express *Dicer*. To examine this, we introduced a shRNA expression plasmid against *Photinus* luciferase, pRNA-U6.1/Neo/siRNA, together with the reporter plasmids carrying the *Photinus* and *Renilla* luciferase genes into C2C12 myoblast and myotubes. The results indicate that the shRNA expression plasmid, or shRNAs can induce RNAi in either C2C12 myoblast or myotube (Fig. 7), suggesting that the Dicer protein could be present in those cells. An interesting point to note is that a decrease in the RNAi activity induced by 0.1 μg pRNA-U6.1/Neo/siRNA was observed in C2C12 myotubes that differentiated for 7 days. This may be caused by a possible decrease in the amounts of Dicer and eIF2C1~4 in the cells. To further evaluate the results and a possible relationship between the quantitative level of either Dicer or eIF2C1~4 and RNAi activity, more extensive studies must be conducted.

Integrity of mammalian RNAi

Our previous study has demonstrated that RNAi activity induced by synthetic siRNA duplexes in post mitotic neurons persists for at least 3 weeks, i.e., a long-lasting RNAi activity occurs in mammalian neurons [29]. Our present and previous studies, therefore, suggest that there is a significant difference in the duration of RNAi activity between muscle and neuron, both of which are terminally differentiated and cell cycle-arrested cells. Since neither muscle nor neuron probably undergoes a decrease in the number of functional RISCs by cell division, it may be possible that the stability of functional RISCs could differ between muscle and neuron.

The present observations further suggest the possibility that a little amount of either Dicer or eIF2C1~4 might be sufficient for activation of mammalian RNAi. This seems to be an important point for understanding mammalian RNAi, and further studies on the contribution of either Dicer or eIF2C1~4 to mammalian RNAi must be conducted.

Finally, all the data presented here lead us to the possibility that RNAi may be applicable for a creation of possible model cells and/or model animals for inherited muscular diseases, for example, muscular dystrophy.

Acknowledgments

We thank Drs. Ojima and Takeda (National Institute of Neuroscience) for their technical advice on the preparation of muscle fibers from mouse extensor digitorum longus. This work was supported in part by a Grant-in-Aid from the Japan Society for the Promotion of Science and by research grants from the Ministry of Health, Labor and Welfare in Japan.

References

[1] P.A. Sharp, RNAi and double-strand RNA, Genes Dev. 13 (1999) 139–141.
[2] J.M. Bosher, M. Labouesse, RNA interference: genetic wand and genetic watchdog, Nat. Cell Biol. 2 (2000) E31–E36.
[3] H. Vaucheret, C. Beclin, M. Fagard, Post-transcriptional gene silencing in plants, J. Cell Sci. 114 (2001) 3083–3091.
[4] H. Cerutti, RNA interference: traveling in the cell and gaining functions?, Trends Genet. 19 (2003) 39–46.
[5] S.M. Hammond, E. Bernstein, D. Beach, G.J. Hannon, An RNA-directed nuclease mediates post-transcriptional gene silencing in *Drosophila* cells, Nature 404 (2000) 293–296.
[6] P.D. Zamore, T. Tuschl, P.A. Sharp, D.P. Bartel, RNAi: double-stranded RNA directs the ATP-dependent cleavage of mRNA at 21 to 23 nucleotide intervals, Cell 101 (2000) 25–33.
[7] E. Bernstein, A.A. Caudy, S.M. Hammond, G.J. Hannon, Role for a bidentate ribonuclease in the initiation step of RNA interference, Nature 409 (2001) 363–366.
[8] S.M. Elbashir, W. Lendeckel, T. Tuschl, RNA interference is mediated by 21- and 22-nucleotide RNAs, Genes Dev. 15 (2001) 188–200.

[9] P. Svoboda, P. Stein, H. Hayashi, R.M. Schultz, Selective reduction of dormant maternal mRNAs in mouse oocytes by RNA interference, Development 127 (2000) 4147–4156.
[10] F. Wianny, M. Zernicka-Goetz, Specific interference with gene function by double-stranded RNA in early mouse development, Nat. Cell Biol. 2 (2000) 70–75.
[11] E. Billy, V. Brondani, H. Zhang, U. Muller, W. Filipowicz, Specific interference with gene expression induced by long, double-stranded RNA in mouse embryonal teratocarcinoma cell lines, Proc. Natl. Acad. Sci. USA 98 (2001) 14428–14433.
[12] S. Yang, S. Tutton, E. Pierce, K. Yoon, Specific double-stranded RNA interference in undifferentiated mouse embryonic stem cells, Mol. Cell. Biol. 21 (2001) 7807–7816.
[13] M.R. Player, P.F. Torrence, The 2-5A system: modulation of viral and cellular processes through acceleration of RNA degradation, Pharmacol. Ther. 78 (1998) 55–113.
[14] M. Gale Jr., M.G. Katze, Molecular mechanisms of interferon resistance mediated by viral-directed inhibition of PKR, the interferon-induced protein kinase, Pharmacol. Ther. 78 (1998) 29–46.
[15] S.M. Elbashir, J. Harborth, W. Lendeckel, A. Yalcin, K. Weber, T. Tuschl, Duplexes of 21-nucleotide RNAs mediate RNA interference in cultured mammalian cells, Nature 411 (2001) 494–498.
[16] S. Matsuda, Y. Ichigotani, T. Okuda, T. Irimura, S. Nakatsugawa, M. Hamaguchi, Molecular cloning and characterization of a novel human gene (HERNA) which encodes a putative RNA-helicase, Biochim. Biophys. Acta 1490 (2000) 163–169.
[17] R.H. Nicholson, A.W. Nicholson, Molecular characterization of a mouse cDNA encoding Dicer, a ribonuclease III ortholog involved in RNA interference, Mamm. Genome 13 (2002) 67–73.
[18] P. Provost, D. Dishart, J. Doucet, D. Frendewey, B. Samuelsson, O. Radmark, Ribonuclease activity and RNA binding of recombinant human Dicer, EMBO J. 21 (2002) 5864–5874.
[19] H. Zhang, F.A. Kolb, V. Brondani, E. Billy, W. Filipowicz, Human Dicer preferentially cleaves dsRNAs at their termini without a requirement for ATP, EMBO J. 21 (2002) 5875–5885.
[20] K.S. Yan, S. Yan, A. Farooq, A. Han, L. Zeng, M.M. Zhou, Structure and conserved RNA binding of the PAZ domain, Nature 426 (2003) 468–474.
[21] J. Martinez, A. Patkaniowska, H. Urlaub, R. Luhrmann, T. Tuschl, Single-stranded antisense siRNAs guide target RNA cleavage in RNAi, Cell 110 (2002) 563–574.
[22] N. Doi, S. Zenno, R. Ueda, H. Ohki-Hamazaki, K. Ui-Tei, K. Saigo, Short-interfering-RNA-mediated gene silencing in mammalian cells requires Dicer and eIF2C translation initiation factors, Curr. Biol. 13 (2003) 41–46.
[23] J.D. Rosenblatt, A.I. Lunt, D.J. Parry, T.A. Partridge, Culturing satellite cells from living single muscle fiber explants, In Vitro Cell. Dev. Biol. Anim. 31 (1995) 773–779.
[24] D. Yaffe, O. Saxel, Serial passaging and differentiation of myogenic cells isolated from dystrophic mouse muscle, Nature 270 (1977) 725–727.
[25] H. Hohjoh, RNA interference (RNAi) induction with various types of synthetic oligonucleotide duplexes in cultured human cells, FEBS Lett. 521 (2002) 195–199.
[26] S.M. Hammond, S. Boettcher, A.A. Caudy, R. Kobayashi, G.J. Hannon, Argonaute2, a link between genetic and biochemical analyses of RNAi, Science 293 (2001) 1146–1150.
[27] R.W. Williams, G.M. Rubin, ARGONAUTE1 is required for efficient RNA interference in *Drosophila* embryos, Proc. Natl. Acad. Sci. USA 99 (2002) 6889–6894.
[28] T. Holen, M. Amarzguioui, M.T. Wiiger, E. Babaie, H. Prydz, Positional effects of short interfering RNAs targeting the human coagulation trigger tissue factor, Nucleic Acids Res. 30 (2002) 1757–1766.
[29] K. Omi, K. Tokunaga, H. Hohjoh, Long-lasting RNAi activity in mammalian neurons, FEBS Lett. 558 (2004) 89–95.

Congestive Heart Failure

Low-dose carvedilol improves left ventricular function and reduces cardiovascular hospitalization in Japanese patients with chronic heart failure: The Multicenter Carvedilol Heart Failure Dose Assessment (MUCHA) trial

Masatsugu Hori, MD, PhD,[a] Shigetake Sasayama, MD, PhD,[b] Akira Kitabatake, MD, PhD,[c] Teruhiko Toyo-oka, MD,[d] Shunnosuke Handa, MD, PhD,[e] Mitsuhiro Yokoyama, MD, PhD,[f] Masunori Matsuzaki, MD, PhD,[g] Akira Takeshita, MD, PhD,[h] Hideki Origasa, PhD,[i] Kennichi Matsui, BA,[j] and Saichi Hosoda, MD, PhD,[k] on behalf of the MUCHA Investigators *Suita, Kyoto, Sapporo, Tokyo, Isehara, Kobe, Ube, Fukuoka, and Toyama, Japan*

Background The efficacy and optimum dose of β-blockers have not been established in Japanese patients with chronic heart failure (CHF). The efficacy and safety of two doses of carvedilol, a β-blocker with vasodilator and antioxidant actions, were investigated in Japanese patients with CHF.

Methods After screening and a carvedilol challenge phase, 174 patients with mild to moderate CHF were randomly assigned (double-blinded) to placebo, 2.5 mg of carvedilol twice daily, or 10 mg of carvedilol twice daily. After a 2- to 4-week uptitration phase, maintenance treatment was continued for 24 to 48 weeks. The primary end point was improvement of the global assessment of CHF by the attending physician. Secondary end points were death or hospitalization for cardiovascular disease, cardiovascular hospitalization, hospitalization for heart failure, change of left ventricular ejection fraction, and change in New York Heart Association class.

Results Carvedilol therapy achieved dose-dependent improvement of all end points (*P* for linear trend, range .002 to <.001). Both carvedilol groups showed marked risk reduction (71% to 91%) for cardiovascular and CHF hospitalization and for death or cardiovascular hospitalization (*P* range, .024 to <.001 for pairwise comparisons with placebo). No significant differences were observed for noncardiovascular hospitalization or adverse events.

Conclusions In Japanese patients with mild or moderate CHF, carvedilol achieved dose-related improvement of CHF and left ventricular ejection fraction; cardiovascular hospitalization was markedly reduced. At 5 mg/d, carvedilol conferred an important patient benefit, less than at 20 mg/d. (Am Heart J 2004;147:324–30.)

See related Editorial on page 200.

A number of double-blind, placebo-controlled, randomized studies performed in the United States and Europe have shown a beneficial effect of β-blockers on mortality and morbidity in patients with chronic heart failure (CHF).[1–5] Carvedilol is a third-generation β-blocker with vasodilatory and antioxidant actions, which has been established as an effective drug for mild to severe CHF. However, a placebo-controlled randomized study of β-blocker therapy has not yet been performed in Japanese patients with CHF.

In Western countries, the recommended initial dose of carvedilol for the treatment of CHF is 6.25 mg/d,

From the [a]Department of Internal Medicine and Therapeutics, Osaka University Graduate School of Medicine, Suita, Japan, the [b]Department of Cardiovascular Medicine, Kyoto University Graduate School of Medicine, Kyoto, Japan, the [c]Department of Cardiovascular Medicine, Hokkaido University Graduate School of Medicine, Sapporo, Japan, the [d]Director of the Medical and Health Care Center, The University of Tokyo Hospital, Tokyo, Japan, the [e]Department of Internal Medicine, Tokai University School of Medicine, Isehara, Japan, the [f]Department of Internal Medicine I, Kobe University School of Medicine, Kobe, Japan, the [g]Department of Internal Medicine II, Yamaguchi University School of Medicine, Ube, Japan, the [h]Coronary Care Unit, Kyusyu University Hospital, Fukuoka, Japan, the [i]Department of Biostatistics, Faculty of Medicine, Toyama Medical and Pharmaceutical University, Toyama, Japan, [j]CMIC Co, Ltd, Tokyo, Japan, and the [k]Director of Sakakibara Heart Institute, Tokyo, Japan.

Supported by Daiichi Pharmaceutical Co, Ltd, and Nippon Roche KK.

The MUCHA committee members are listed in the Appendix.

Submitted March 18, 2003; accepted July 29, 2003.

Reprint requests: Masatsugu Hori, MD, PhD, Department of Internal Medicine and Therapeutics, Osaka University Graduate School of Medicine, 2-2 Yamada-oka, Suita, Osaka 565-0871, Japan.
E-mail: mhori@medone.med.osaka-u.ac.jp

0002-8703/$ - see front matter

doi:10.1016/j.ahj.2003.07.023

Table I. Baseline characteristics of the 3 randomized groups

Parameter	Placebo group (n = 49)	5 mg Group (n = 47)	20 mg Group (n = 77)	P
Age (y)	62 ± 12	59 ± 9	60 ± 12	.581*
Sex (male/female) (%)	82/18	77/23	74/26	.613†
Etiology of heart failure				
Nonischemic/ischemic (%)	76/24	75/25	71/29	.864†
NYHA class, II/III (%)	80/20	81/19	75/25	.735†
LVEF (%)	29 ± 7	30 ± 8	30 ± 7	.734*
Systolic BP (mm Hg)	121 ± 17	117 ± 16	119 ± 14	.418*
Diastolic BP (mm Hg)	72 ± 11	72 ± 11	73 ± 10	.660*
Heart rate (beats/min)	81 ± 14	74 ± 11	78 ± 17	.097*
Body weight (kg)	60 ± 10	60 ± 11	62 ± 14	.349*
Other medications				
ACE inhibitors (%)	80	81	70	.304†
Diuretics (%)	84	85	88	.743†
Digitalis (%)	59	70	65	.527†

Values presented as mean ± SD.
*Regression analysis.
†χ^2 Test.

followed by uptitration to 50 mg/d for maintenance treatment if tolerated.[6] In Japan, the dose of carvedilol for the treatment of hypertension and angina pectoris is 10 to 20 mg/d,[7,8] which is less than half of that used in Western countries. However, the effectiveness of such a low-dose carvedilol regimen for Japanese patients with CHF remains unclear. The present study was designed to test the efficacy and safety of low-dose carvedilol regimens in Japanese patients with CHF.

Methods

Study design

The Multicenter Carvedilol Heart Failure Dose Assessment (MUCHA) trial was a randomized, multicenter, placebo-controlled, double-blinded study conducted in 5 phases: (1) screening, (2) challenge, (3) uptitration, (4) maintenance, and (5) downtitration. During the challenge phase after screening, eligible patients received open-label carvedilol (1.25 mg twice daily) for 1 to 2 weeks, and the dose was increased to 2.5 mg twice daily if tolerated. Patients were entered into the double-blinded uptitration phase after tolerating a dose of 2.5 mg twice daily for at least 2 weeks and were randomly assigned to placebo, carvedilol at 2.5 mg twice daily (5 mg group), or carvedilol at 10 mg twice daily (20 mg group) in the proportion of 1:1:2 by the dynamic allocation method. In the 20 mg group, the carvedilol dose was increased stepwise in a double-blinded fashion at 1- or 2-week intervals to reach 10 mg twice daily or the maximum tolerated dose of <10 mg twice daily. Patients then received placebo or carvedilol at a fixed dose for 24 to 48 weeks during the maintenance phase. When the last entered patient had completed 24 weeks of maintenance therapy, all patients were shifted into the downtitration phase.

Figure 1

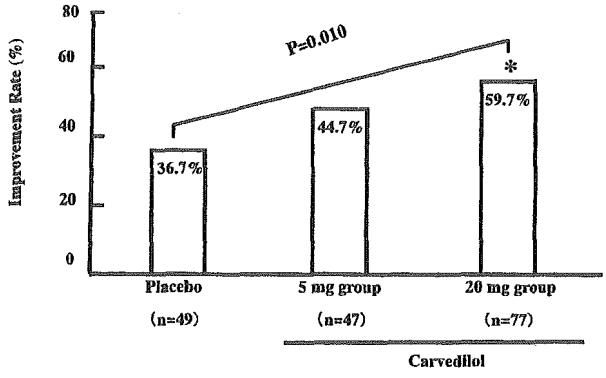

Improvement rate in each group. Improvement rate is the percentage of patients with moderate or marked improvement of signs and symptoms of heart failure as assessed by the attending physician at the end of the maintenance phase in comparison with baseline. Improvement achieved with carvedilol treatment was evaluated by the Cochrane-Armitage test to assess the dose-response relation; pairwise comparisons with placebo were performed by means of χ^2 test. *$P < .05$ vs placebo.

Inclusion and exclusion criteria

Patients who had ischemic or nonischemic cardiomyopathy with stable symptoms (New York Heart Association functional class [NYHA class] II or III) were eligible for enrollment if their left ventricular ejection fraction (LVEF) was ≤40% (measured by M-mode echocardiography or radionuclide ventriculography at the qualifying examination) and

Table II. Death and CVD hospitalization

Parameter	Placebo group (n = 49)	5 mg Group (n = 47)	20 mg Group (n = 77)	Placebo vs 5 mg Hazard ratio [95% CI]	Placebo vs 5 mg P*	Placebo vs 20 mg Hazard ratio [95% CI]	Placebo vs 20 mg P	P for linear trend†
Death or CVD hospitalization (%)	12 (24.5)	4 (8.5)	4 (5.2)	0.29 [0.10–0.91]	.024	0.20 [0.06–0.60]	.002	.002
CVD hospitalization (%)	12 (24.5)	2 (4.3)	3 (3.9)	0.14 [0.03–0.65]	.003	0.15 [0.04–0.52]	<.001	<.001
Worsening CHF	10 (20.4)	1 (2.1)	2 (2.6)	0.09 [0.01–0.69]	.004	0.12 [0.03–0.54]	<.001	<.001
Other CDV reasons	3 (6.1)	1 (2.1)	1 (1.3)	0.29 [0.03–2.75]	.229	0.20 [0.021–1.88]	.116	.111

*Log-rank test.
†Linear trend test using the Cox proportional hazards regression model.

Figure 2

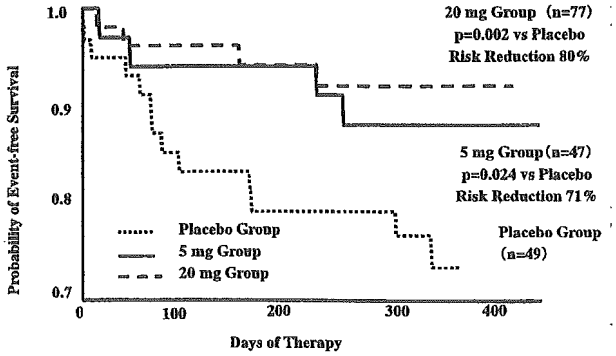

Kaplan-Meier analysis of the probability of survival without death or CVD hospitalization in patients randomly assigned to placebo (*dotted line*), 5 mg/d carvedilol (*solid line*), or 20 mg/d carvedilol (*broken line*). Graph shows time to first event for each group. Dose-response relation was analyzed by means of Cox proportional hazards regression model; log-rank test was used to compare each carvedilol dose with placebo.

their age was between 20 and 79 years. Patients with the following conditions were excluded: valvular heart disease, hypertrophic obstructive cardiomyopathy, cardiogenic shock, systolic blood pressure <90 mm Hg, bradycardia (<60/min), grade II or III atrioventricular block, life-threatening arrhythmia, unstable angina, resting angina, cor pulmonale, asthma, Raynaud phenomenon, and intermittent claudication. Patients were also excluded if myocardial infarction or coronary artery bypass grafting had occurred within the preceding 3 months.

Diuretics, digitalis, angiotensin-converting enzyme (ACE) inhibitors, calcium channel blockers, vasodilators, and antiarrhythmic agents could be used concomitantly. Drugs prohibited during the study were other β-blockers, αβ-blockers, α-blockers, inotropic agents other than digitalis, and intravenous diltiazem hydrochloride or verapamil hydrochloride.

The institutional review board of each participating hospital approved the study, and each subject gave written informed consent.

Parameters assessed

The primary end point of the study was improvement of the global assessment of CHF (signs and symptoms) by the attending physician. The secondary end points were as follows: all-cause death or hospitalization for cardiovascular disease (CVD), CVD hospitalization, hospitalization for worsening CHF, changes of LVEF, and changes of NYHA class.

Global assessment of heart failure was performed by entering CHF symptoms and objective findings at baseline and follow-up into a study form. Differences between the assessment at baseline and at last follow-up during maintenance treatment were rated according to the protocol and were assigned one of the following 6 grades: markedly improved, moderately improved, mildly improved, no change, worsened, or unassessable. The improvement rate (the primary end point) for each treatment group was defined as the proportion assigned a rating of "moderately improved" or "markedly improved." Data concerning CVD hospitalizations and deaths were reported prospectively by the investigators and were reviewed and classified by the End Point Committee.

The end point of changes in LVEF was defined as the difference between M-mode echocardiography measurements at baseline and last follow-up during the maintenance phase, with the left ventricular volumes being calculated by the method of Teichholz. The Data and Safety Monitoring Board prospectively monitored all serious adverse events.

Statistical analysis

On the basis of data from a Japanese pilot study and the US Carvedilol Heart Failure Trials Program,[9-12] it was projected that a sample size of 160 patients (40 for the placebo group, 40 for the 5 mg group, and 80 for the 20 mg group) would provide 80% power at the $P = .05$ level of significance to detect a dose-response effect among the three groups as well as assessing the efficacy of each carvedilol dose.

Data on the improvement rate from the physicians' global assessments were analyzed by the Cochrane-Armitage test to

Table III. Death or CVD hospitalization rates according to baseline characteristics

Subgroup	Event rate (%) Placebo group (P)	5 mg Group (L)	20 mg Group (H)	*P*, linear trend test*	Hazard ratio (*P*, Log-rank test) P vs L	P vs H
Sex						
Male (n = 133)	25.0	8.3	7.0	.013	0.27 (.036)	0.26 (.015)
Female (n = 40)	22.2	9.1	0.0	.034	0.39 (.419)	– (.023)
Age (y)						
<65 (n = 99)	24.0	0.0	4.4	.014	– (.005)	0.21 (.019)
≥65 (n = 74)	25.0	22.2	6.3	.041	0.81 (.745)	0.21 (.032)
Etiology						
Nonischemic (n = 127)	24.3	2.9	3.6	.002	0.10 (.007)	0.15 (.005)
Ischemic (n = 46)	25.0	25.0	9.1	.150	0.84 (.829)	0.29 (.156)
NYHA class						
II (n = 135)	28.2	7.9	6.9	.005	0.23 (.013)	0.23 (.006)
III (n = 38)	10.0	11.1	0.0	.215	1.05 (.970)	– (.180)
LVEF (%)						
<30 (n = 76)	33.3	10.0	2.9	.002	0.25 (.059)	0.08 (.003)
≥30 (n = 95)	18.5	7.4	7.3	.140	0.35 (.192)	0.34 (.127)
Systolic BP (mm Hg)						
<120 (n = 84)	15.0	14.8	10.8	.638	0.95 (.950)	0.70 (.633)
≥120 (n = 89)	31.0	0.0	0.0	<.001	– (.004)	– (.001)
Heart rate (beats/min)						
<75 (n = 78)	29.4	11.1	8.8	.102	0.35 (.135)	0.31 (.089)
≥75 (n = 95)	21.9	5.0	2.3	.004	0.18 (.073)	0.09 (.005)

*Linear trend test using the Cox proportional hazards regression model.

Table IV. Death or CVD hospitalization rates according to presence of concomitant disease at baseline examination

Subgroup	Event rate (%) Placebo group (P)	5 mg Group (L)	20 mg Group (H)	*P*, linear trend test*	Hazard ratio (*P*, Log-rank test) P vs L	P vs H
Hypertension						
Nonhypertensive (n = 132)	22.9	10.3	5.2	.014	0.38 (.104)	0.22 (.013)
Hypertensive (n = 41)	28.6	0.0	5.3	.041	– (.104)	0.15 (.052)
Diabetes						
Nondiabetic (n = 118)	24.2	6.1	7.7	.035	0.21 (.031)	0.30 (.035)
Diabetic (n = 55)	25.0	14.3	0.0	.011	0.49 (.401)	–(.010)
Hyperlipidemia						
Normolipidemic (n = 136)	26.8	8.6	6.7	.007	0.28 (.037)	0.24 (.008)
Hyperlipidemic (n = 37)	12.5	8.3	0.0	.140	0.53 (.648)	– (.145)
Cardiac rhythm						
Sinus rhythm (n = 132)	21.4	11.4	1.8	.002	0.46 (.188)	0.08 (.002)
Atrial fibrillation (n = 41)	42.9	0.0	13.6	.214	– (.014)	0.29 (.106)

*Linear trend test using the Cox proportional hazards regression model.

assess the dose-response relation. When a significant difference was found, pairwise comparisons with placebo were performed with the χ^2 test.

For death or CVD hospitalization, CVD hospitalization, and hospitalization for CHF, Kaplan-Meier curves were constructed as time-to-first event plots for each group, and data were analyzed to detect a dose-response relation by means of the Cox proportional hazards regression model. Then event-free survival curves were compared among the placebo group and carvedilol groups by means of the log-rank

Table V. Change of NYHA class from baseline to the end of the maintenance phase

Group	Improved, n (%)	No change, n (%)	Worsened, n (%)	P, Wilcoxon rank sum test	P, linear trend test*
Placebo	23 (48.9)	19 (40.4)	5 (10.6)		
5 mg	38 (80.9)	8 (17.0)	1 (2.1)	.037†	.046
20 mg	51 (70.8)	20 (27.8)	1 (1.4)	.051†	

*Linear trend test using the Cochrane-Mantel-Haenszel test.
†Versus placebo.

Figure 3

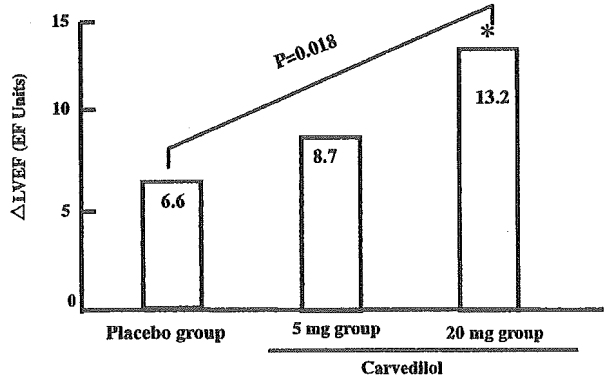

Changes of LVEF from baseline to end of maintenance phase. Dose-response relation was assessed by means of regression analysis; pairwise comparisons with placebo were done by Student *t* test. Change of LVEF was defined as the difference between baseline value and value at end of maintenance phase and is expressed in ejection fraction (EF) units.

test. All analyses were performed on the full analysis set,[13] and the level of significance was set at $P < .05$ (2-tailed).

Results

Open-label challenge phase

Treatment was started on October 28, 1996, and the trial was completed on March 17, 2000. One hundred ninety patients commenced the challenge phase and 174 patients (91.6%) were randomly assigned to the 3 treatment groups.

Baseline patient profile

Of 174 patients randomly assigned to the 3 treatment groups, one patient in the 20 mg group who received no study medication was excluded from the full analysis set. There were no significant differences in baseline characteristics among the three treatment groups (Table I). Seventy-four percent of patients in the 20 mg group and 100% in the 5 mg group achieved the target dose; the mean dose was 17.2 mg/d in the 20 mg group.

Global assessment of changes in CHF (primary end point)

The percentage of each treatment group with moderate or marked improvement in signs and symptoms of heart failure (improvement rate) ascertained by attending physicians showed a significant dose-response relation to carvedilol ($P = .010$), and in pairwise comparison, the improvement rate was significantly higher in the 20 mg group than in the placebo group ($P = .012$) (Figure 1).

Death or CVD hospitalization

The incidence of death or CVD hospitalization showed a significant dose-response relation ($P = .002$) and was significantly lower in both the 5 mg group ($P = .024$) and the 20 mg group ($P < .002$) on pairwise comparison with the placebo group (Table II and Figure 2). Risk reduction was 71% in the 5 mg group and 80% in the 20 mg group. Carvedilol treatment was associated with a highly significant decrease of the CVD hospitalization rate in the 5 mg group ($P = .003$) and the 20 mg group ($P < .001$), as well as for the linear trend ($P < .001$). Compared with placebo, the reduction in risk of CVD hospitalization was 86% in the 5 mg group and 85% in the 20 mg group (Table II). This included a risk reduction for hospitalization resulting from worsening heart failure of 91% for the 5 mg group and 88% for the 20 mg group.

Subgroup analysis showed that the risk of death or CVD hospitalization was lower in the carvedilol-treated groups regardless of age, sex, underlying cause of CHF, severity of CHF, LVEF, systolic blood pressure, or heart rate (Table III). The risk of death or CVD hospitalization in high-risk patients with hypertension, diabetes mellitus, hyperlipidemia, and atrial fibrillation was also lower in the carvedilol-treated groups (Table IV).